High-momentum proton removal from ^{16}O and the $(e,e'p)$ cross section

A. Polls

Departament d'Estructura i Constituents de la Matèria, Universitat de Barcelona, Diagonal 647, E-8028 Barcelona, Spain

M. Radici and S. Boffi

Dipartimento di Fisica Nucleare e Teorica, Università di Pavia, and Istituto Nazionale di Fisica Nucleare,
Sezione di Pavia, I-27100 Pavia, Italy

W. H. Dickhoff

Department of Physics, Washington University, St. Louis, Missouri 63130

H. Müther

Institut für Theoretische Physik, Universität Tübingen, Auf der Morgenstelle 14, D-72076 Tübingen, Germany

The cross section for the removal of high-momentum protons from ^{16}O is calculated for high missing energies. The admixture of high-momentum nucleons in the ^{16}O ground state is obtained by calculating the single-hole spectral function directly in the finite nucleus with the inclusion of short-range and tensor correlations induced by a realistic meson-exchange interaction. The presence of high-momentum nucleons in the transition to final states in ^{15}N at 60–100 MeV missing energy is converted to the coincidence cross section for the $(e,e'p)$ reaction by including the coupling to the electromagnetic probe and the final state interactions of the outgoing proton in the same way as in the standard analysis of the experimental data. Detectable cross sections for the removal of a single proton at these high missing energies are obtained which are considerably larger at higher missing momentum than the corresponding cross sections for the p-wave quasihole transitions. Cross sections for these quasihole transitions are compared with the most recent experimental data available. [S0556-2813(97)03902-2]

I. INTRODUCTION

Experimental progress in the exclusive $(e,e'p)$ reaction in recent years has provided a clear picture of the limitations of the simple shell-model description of closed-shell nuclei. Of particular interest is the reduction of the single-particle (sp) strength for the removal of particles with valence hole quantum numbers with respect to the simple shell-model estimate which corresponds to a spectroscopic factor of 1 for such states. Typical experimental results [1] for closed-shell nuclei exhibit reductions of about 30–45% for these spectroscopic factors. In the case of ^{208}Pb, one obtains a spectroscopic factor for the transition to the ground state of ^{207}Tl of about 0.65 which is associated with the removal of a $3s\frac{1}{2}$ proton. An analysis which uses information obtained from elastic electron scattering indicates that the total occupation number for this state is about 10% higher [2], corresponding to 0.75. This additional background strength should be present at higher missing energy and is presumed to be highly fragmented. The depletion of more deeply bound orbitals is expected to be somewhat less as suggested by theoretical considerations [3] which also indicate that the strength in the background, outside the main peak, corresponds to about 10% (see also [4]).

Recent experimental results for ^{16}O [5] yield a combined quasihole strength for the $p\frac{1}{2}$ and $p\frac{3}{2}$ states corresponding to about 65% with the $p\frac{1}{2}$ strength concentrated in one peak and the $p\frac{3}{2}$ strength fragmented already over several peaks. Recent theoretical results yield about 76% for these p states [6]

without reproducing the fragmentation of the $p\frac{3}{2}$ strength. This calculation includes the influence of both long-range correlations, associated with a large shell-model space, as well as short-range correlations. This inclusion of the long-range correlations yields in general a good description of, e.g., the $l=2$ strength. However, it fails to reproduce some details: In the experimental data, one observes some strength of positive parity ($l=2$) at energies below the first $p\frac{3}{2}$ fragment whereas the calculation yields all $l=2$ strength above the $p\frac{3}{2}$ peak. This suggests that additional work has to be done to reproduce such details. Furthermore, one should be aware that also a correct treatment of the center-of-mass motion may affect the distribution of single-particle strength even for nuclei as heavy as ^{16}O [7]. The contribution to the depletion of the sp strength due to short-range correlations is typically about 10%. This result is obtained both in nuclear matter calculations, as reviewed in [3], and in calculations directly for finite (medium) heavy nuclei [7–10,6]. Although the influence of long-range correlations on the distribution of the sp strength is substantial, it is clear that a sizable fraction of the missing sp strength is due to short-range effects. The experimental data [1,5] indicate that only about 70% of the expected protons in the nucleus has been detected in the energy and momentum domain studied so far. It is therefore important to establish precisely where the protons which have been admixed into the nuclear ground state due to short-range and tensor correlations can be detected in the $(e,e'p)$ reaction and with what cross section.

The influence of short-range correlations on the presence

of high-momentum components in finite (medium) heavy nuclei has been calculated in [8–10]. In this work the spectral function for ^{16}O has been calculated from a realistic interaction without recourse to some form of local density approximation [11,12]. No substantial high-momentum components are obtained in [8–10] at small missing energy. With increasing missing energy, however, one recovers the high-momentum components which have been admixed into the ground state. The physics of these features can be traced back to the realization that the admixture of high momenta requires the coupling to two-hole–one-particle (2h1p) states in the self-energy for a nucleon with high momentum. In nuclear matter the conservation of momentum requires the equality of the 2h1p momentum in the self-energy and the external high momentum. Since the two-hole state has a relatively small total pair momentum, one automatically needs an essentially equally large and opposite momentum for the intermediate one-particle state to fulfill momentum conservation. As a result, the relevant intermediate 2h1p states will lie at increasing excitation energy with increasing momentum. Considerations of this type are well known for nuclear matter (see, e.g., [13]), but are approximately valid in finite nuclei as well. Recent experiments on ^{208}Pb [14] and ^{16}O [15] essentially confirm that the presence of high-momentum components in the quasihole states accounts for only a tiny fraction of the sp strength.

The theoretical prediction concerning the presence of high-momentum components at high missing energy remains to be verified experimentally, however. In order to facilitate and support these efforts, the present work aims to combine the calculation of the spectral function at these energies with the description of both the electromagnetic vertex and final state interactions (FSI's) in order to produce realistic estimates of the exclusive $(e,e'p)$ cross section under experimental conditions possible at NIKHEF and Mainz. The impulse approximation has been adopted for the electromagnetic current operator, which describes the nonrelativistic reduction (up to fourth order in the inverse nucleon mass [16]) of the coupling between the external virtual photon and single nucleons only. The treatment of FSI's has been developed by the Pavia group [17–21] (see also Ref. [22]) and takes into account the average complex optical potential the nucleon experiences on its way out of the nucleus. Other contributions to the exclusive $(e,e'p)$ reaction are present in principle, such as two-step mechanisms in the final state or the decay of initial collective excitations in the target nucleus. However, by transferring sufficiently high energy ω to the target nucleus and by selecting typical kinematical conditions corresponding to the so-called quasielastic peak with $\omega = q^2/2m$ (q the momentum transfer and m the nucleon mass), these contributions are suppressed. In these conditions, adopted in the most recent experiments, the direct knockout mechanism has been shown to be the dominant contribution [21] and essentially corresponds to calculating the combined probability for exciting a correlated particle (which is ultimately detected) and a correlated hole such that energy and momentum are conserved but no further interaction of the particle with the hole is included.

The calculation of the spectral function for ^{16}O is reviewed in Sec. II. Special attention is given to a separable representation of the spectral function which facilitates the

practical implementation of the inclusion of FSI's. In Sec. III the general formalism of the distorted wave impulse approximation (DWIA) is briefly reviewed. The influence of FSI's is studied in Sec. IV for the quasihole transitions for which data are available [5,15]. Extending the calculation of the cross section to higher missing energies yields the expected rise of high-missing-momentum components in the cross section in comparison to the results near the Fermi energy. The contribution of various partial waves is studied demonstrating the increasing importance of higher l values with increasing missing momentum. All these results are discussed in Sec. IV and a brief summary is presented in Sec. V.

II. SINGLE-PARTICLE SPECTRAL FUNCTION

The calculation of the cross section for exclusive $(e,e'p)$ processes requires the knowledge of the hole spectral function which is defined in the following way

$$S(\mathbf{p},m_s,m_\tau,\mathbf{p}',m_s',m_\tau;E)$$

$$= \sum_n \langle \Psi_0^A | a^\dagger(\mathbf{p}',m_s',m_\tau) | \Psi_n^{A-1} \rangle$$

$$\times \langle \Psi_n^{A-1} | a(\mathbf{p},m_s,m_\tau) | \Psi_0^A \rangle \delta(E - (E_0^A - E_n^{A-1})), \quad (1)$$

where the summation over n runs over the discrete excited states as well as over the continuum of the $(A-1)$ particle system, $|\Psi_0^A\rangle$ is the ground state of the initial nucleus, and $a(\mathbf{p},m_s,m_\tau)$ $[a^\dagger(\mathbf{p}',m_s',m_\tau)]$ is the annihilation [creation] operator with the specified sp quantum numbers for momenta and third component of spin and isospin, respectively. The spectral function is diagonal in the third component of the isospin, and ignoring the Coulomb interaction between the protons, the spectral functions for protons and neutrons are identical for $N=Z$ nuclei. Therefore in the following we have dropped the isospin quantum number m_τ. Note that the energy variable E in this definition of the spectral function refers to minus the excitation energy of state n in the $A-1$ particle system with respect to the ground-state energy (E_0^A) of the nucleus with A nucleons.

To proceed further in the calculations it is useful to introduce a partial wave decomposition which yields the spectral function for a nucleon in the sp basis with orbital angular momentum l, total angular momentum j, and momentum p:

$$S_{lj}(p,p';E) = \sum_n \langle \Psi_0^A | a_{p'lj}^\dagger | \Psi_n^{A-1} \rangle \langle \Psi_n^{A-1} | a_{plj} | \Psi_0^A \rangle$$

$$\times \delta(E - (E_0^A - E_n^{A-1})), \quad (2)$$

where a_{plj} $(a_{p'lj}^\dagger)$ denotes the corresponding removal (addition) operator. The spectral functions for the various partial waves, $S_{lj}(p,p';E)$, have been obtained from the imaginary part of the corresponding sp propagator $g_{lj}(p,p';E)$. This Green's function solves the Dyson equation
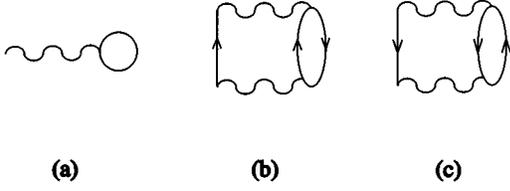
FIG. 1. Graphical representation of the Hartree-Fock (a), the two-particle–one-hole (2p1h) (b), and the two-hole–one-particle contribution (2h1p) (c), to the self-energy of the nucleon.

$$g_{lj}(p_1,p_2;E) = g_{lj}^{(0)}(p_1,p_2;E) + \int dp_3 \int dp_4 g_{lj}^{(0)}$$
$$\times (p_1,p_3;E) \Delta\Sigma_{lj}(p_3,p_4;E) g_{lj}(p_4,p_2;E),$$
$$(3)$$

where $g^{(0)}$ refers to a Hartree-Fock propagator and $\Delta\Sigma_{lj}$ represents contributions to the real and imaginary parts of the irreducible self-energy, which go beyond the Hartree-Fock approximation of the nucleon self-energy used to derive $g^{(0)}$. Although the evaluation of the self-energy as well as the solution of the Dyson equation has been discussed in detail in previous publications [9,10], we include here a brief summary of the relevant aspects of the method.

A. Calculation of the nucleon self-energy

The self-energy is evaluated in terms of a G matrix which is obtained as a solution of the Bethe-Goldstone equation for nuclear matter choosing for the bare NN interaction the one-boson-exchange potential B defined by Machleidt (Ref. [23], Table A.2). We have chosen version B as it seems to be the most typical of the different Bonn potentials. The strength of its tensor components is in between those of versions A and C as can be seen from the d-state probabilities calculated for the deuteron (4.5 for Bonn A, 5.1 for Bonn B, and 5.5 for Bonn C). The Bethe-Goldstone equation has been solved for a Fermi momentum $k_F = 1.4$ fm^{-1} and starting energy -10 MeV. The choices for the density of nuclear matter and the starting energy are rather arbitrary. It turns out, however, that the calculation of the Hartree-Fock term [Fig. 1(a)] is not very sensitive to this choice [24]. Furthermore, we will correct this nuclear matter approximation by calculating the two-particle–one-hole (2p1h) term displayed in Fig. 1(b) directly for the finite system. This second-order correction, which assumes harmonic oscillator states for the occupied (hole) states and plane waves for the intermediate unbound particle states, incorporates the correct energy and density dependence characteristic of a finite nucleus G matrix. To evaluate the diagrams in Fig. 1, we need matrix elements in a mixed representation of one particle in a bound harmonic oscillator while the other is in a plane wave state. Using vector bracket transformation coefficients [25] one can transform matrix elements from the representation in coordinates of relative and center-of-mass momenta to the coordinates of sp momenta in the laboratory frame in which the two-particle state is described by

$$|p_1 l_1 j_1 p_2 l_2 j_2 JT\rangle, \qquad (4)$$

where p_i, l_i, and j_i refer to momentum and angular momenta of particle i whereas J and T define the total angular momentum and isospin of the two-particle state. Performing an integration over one of the p_i, one obtains a two-particle state in the mixed representation

$$|n_1 l_1 j_1 p_2 l_2 j_2 JT\rangle = \int_0^\infty dp_1 p_1^2 R_{n_1,l_1}(\alpha p_1)|p_1 l_1 j_1 p_2 l_2 j_2 JT\rangle. \qquad (5)$$

Here R_{n_1,l_1} stands for the radial oscillator function and the oscillator length $\alpha = 1.72$ fm^{-1} has been chosen to have an appropriate description of the bound sp states in ^{16}O. Using the notation defined in Eqs. (4) and (5), our Hartree-Fock approximation for the self-energy is obtained in the momentum representation

$$\Sigma_{l_1 j_1}^{\mathrm{HF}}(p_1,p_1') = \frac{1}{2(2j_1+1)} \sum_{n_2 l_2 j_2 JT} (2J+1)(2T+1)$$
$$\times \langle p_1 l_1 j_1 n_2 l_2 j_2 JT|G|p_1' l_1 j_1 n_2 l_2 j_2 JT\rangle. \qquad (6)$$

The summation over the oscillator quantum numbers is restricted to the states occupied in the independent particle model of ^{16}O. This Hartree-Fock part of the self-energy is real and does not depend on the energy.

The terms of lowest order in G which give rise to an imaginary part in the self-energy are represented by the diagrams displayed in Figs. 1(b) and 1(c), referring to intermediate 2p1h and 2h1p states, respectively. The 2p1h contribution to the imaginary part is given by

$$W_{l_1 j_1}^{2p1h}(p_1,p_1';E) = \frac{-1}{2(2j_1+1)} \sum_{n_2 l_2 j_2} \sum_{lL} \sum_{JJ_S ST} \int k^2 dk$$
$$\times \int K^2 dK (2J+1)(2T+1)$$
$$\times \langle p_1 l_1 j_1 n_2 l_2 j_2 JT|G|klSJ_S KLT\rangle$$
$$\times \langle klSJ_S KLT|G|p_1' l_1 j_1 n_2 l_2 j_2 JT\rangle_\pi$$
$$\times \delta\left(E + \epsilon_{n_2 l_2 j_2} - \frac{K^2}{4m} - \frac{k^2}{m}\right), \qquad (7)$$

where the ''experimental'' sp energies $\epsilon_{n_2 l_2 j_2}$ are used for the hole states (-47 MeV, -21.8 MeV, and -15.7 MeV for $s\frac{1}{2}$, $p\frac{3}{2}$, and $p\frac{1}{2}$ states, respectively), while the energies of the particle states are given in terms of the kinetic energy only. The plane waves associated with the particle states in the intermediate states are properly orthogonalized to the bound sp states following the techniques discussed by Borromeo et al. [26]. The 2h1p contribution to the imaginary part $W_{l_1 j_1}^{2h1p}(p_1,p_1';E)$ can be calculated in a similar way (see also [26]).

Our choice to assume pure kinetic energies for the particle states in calculating the imaginary parts of W^{2p1h} [Eq. (7)] and W^{2h1p} may not be very realistic for the excitation modes at low energy. Indeed a sizable imaginary part in W^{2h1p} is obtained only for energies E below -40 MeV. As we are

mainly interested, however, in the effects of short-range correlations, which lead to excitations of particle states with high momentum, the choice seems to be appropriate. A different approach would be required to treat the coupling to the very low-lying 2p1h and 2h1p states in an adequate way. Attempts at such a treatment can be found in Refs. [27–31,6]. The 2p1h contribution to the real part of the self-energy can be calculated from the imaginary part W^{2p1h} using a dispersion relation [32]

$$V^{2p1h}_{l_1 j_1}(p_1, p'_1; E) = \frac{1}{\pi} \mathcal{P} \int_{-\infty}^{\infty} \frac{W^{2p1h}_{l_1 j_1}(p_1, p'_1; E')}{E' - E} dE', \quad (8)$$

where $\mathcal{P}$ represents a principal value integral. A similar dispersion relation holds for V^{2h1p} and W^{2h1p}.

Since the Hartree-Fock contribution Σ^{HF} has been calculated in terms of a nuclear matter G matrix, it already contains 2p1h terms of the kind displayed in Fig. 1(b). In order to avoid such an overcounting of the particle-particle ladder terms, we subtract from the real part of the self-energy a correction term (V_c), which just contains the 2p1h contribution calculated in nuclear matter. Summing up the various contributions we obtain for the self-energy the expressions

$$\Sigma = \Sigma^{HF} + \Delta\Sigma = \Sigma^{HF} + (V^{2p1h} - V_c + V^{2h1p})$$
$$+ (W^{2p1h} + W^{2h1p}). \quad (9)$$

B. Solution of the Dyson equation

The next step is to solve the Dyson equation (3) for the sp propagator. To this aim, we discretize the integrals in this equation by considering a complete basis within a spherical box of a radius R_{box}. The calculated observables are independent of the choice of R_{box}, if it is chosen to be around 15 fm or larger. A complete and orthonormal set of regular basis functions within this box is given by

$$\Phi_{iljm}(\mathbf{r}) = \langle \mathbf{r} | p_i l j m \rangle = N_{il} j_l(p_i r) \mathcal{Y}_{ljm}(\theta, \phi). \quad (10)$$

In this equation $\mathcal{Y}_{ljm}$ represent the spherical harmonics including the spin degrees of freedom and j_l denote the spherical Bessel functions for the discrete momenta p_i which fulfill

$$j_l(p_i R_{box}) = 0. \quad (11)$$

Note that the basis functions defined for discrete values of the momentum p_i within the box differ from the plane wave states defined in the continuum with the corresponding momentum just by the normalization constant, which is $\sqrt{2/\pi}$ for the latter. This enables us to determine the matrix elements of the nucleon self-energy in the basis of Eq. (10) from the results presented in the preceding subsection.

As a first step we determine the Hartree-Fock approximation for the sp Green's function in the "box basis." For that purpose the Hartree–Fock Hamiltonian is diagonalized:

$$\sum_{n=1}^{N_{max}} \left\langle p_i \left| \frac{p_i^2}{2m} \delta_{in} + \Sigma^{HF}_{lj} \right| p_n \right\rangle \langle p_n | \alpha \rangle_{lj} = \epsilon^{HF}_{\alpha lj} \langle p_i | \alpha \rangle_{lj}. \quad (12)$$

Here and in the following the set of basis states in the box has been truncated by assuming an appropriate N_{max}. In the basis of Hartree–Fock states $|\alpha\rangle$, the Hartree-Fock propagator is diagonal and given by

$$g^{(0)}_{lj}(\alpha; E) = \frac{1}{E - \epsilon^{HF}_{\alpha lj} \pm i\eta}, \quad (13)$$

where the sign in front of the infinitesimal imaginary quantity $i\eta$ is positive (negative) if $\epsilon^{HF}_{\alpha lj}$ is above (below) the Fermi energy. With these ingredients one can solve the Dyson equation (3). One possibility is to determine first the so-called reducible self-energy, originating from an iteration of $\Delta\Sigma$, by solving

$$\langle \alpha | \Sigma^{red}_{lj}(E) | \beta \rangle = \langle \alpha | \Delta\Sigma_{lj}(E) | \beta \rangle + \sum_{\gamma} \langle \alpha | \Delta\Sigma_{lj}(E) | \gamma \rangle$$
$$\times g^{(0)}_{lj}(\gamma; E) \langle \gamma | \Sigma^{red}_{lj}(E) | \beta \rangle \quad (14)$$

and obtain the propagator from

$$g_{lj}(\alpha, \beta; E) = \delta_{\alpha, \beta} g^{(0)}_{lj}(\alpha; E) + g^{(0)}_{lj}(\alpha; E) \langle \alpha | \Sigma^{red}_{lj}(E) | \beta \rangle$$
$$\times g^{(0)}_{lj}(\beta; E). \quad (15)$$

Using this representation of the Green's function one can calculate the spectral function in the "box basis" from

$$\widetilde{S}^c_{lj}(p_m, p_n; E) = \frac{1}{\pi} \text{Im}\left(\sum_{\alpha, \beta} \langle p_m | \alpha \rangle_{lj} g_{lj}(\alpha, \beta; E) \langle \beta | p_n \rangle_{lj} \right). \quad (16)$$

For energies E below the lowest sp energy of a given Hartree-Fock state (with lj) this spectral function is different from zero only due to the imaginary part in Σ^{red}. This contribution involves the coupling to the continuum of 2h1p states and is therefore nonvanishing only for energies at which the corresponding irreducible self-energy $\Delta\Sigma$ has a nonzero imaginary part. Besides this continuum contribution, the hole spectral function also receives contributions from the quasihole states [9]. The energies and wave functions of these quasihole states can be determined by diagonalizing the Hartree-Fock Hamiltonian plus $\Delta\Sigma$ in the "box basis":

$$\sum_{n=1}^{N_{max}} \left\langle p_i \left| \frac{p_i^2}{2m} \delta_{in} + \Sigma^{HF}_{lj} + \Delta\Sigma_{lj}(E = \epsilon^{qh}_{Ylj}) \right| p_n \right\rangle \langle p_n | Y \rangle_{lj}$$
$$= \epsilon^{qh}_{Ylj} \langle p_i | Y \rangle_{lj}. \quad (17)$$

Since in the present work $\Delta\Sigma$ only contains a sizable imaginary part for energies E below ϵ^{qh}_Y, the energies of the quasihole states are real and the continuum contribution to the spectral function is separated in energy from the quasihole contribution. The quasihole contribution to the hole spectral function is given by

$$\widetilde{S}^{qh}_{Ylj}(p_m, p_n; E) = Z_{Ylj} \langle p_m | Y \rangle_{lj} \langle Y | p_n \rangle_{lj} \delta(E - \epsilon^{qh}_{Ylj}), \quad (18)$$

with the spectroscopic factor for the quasihole state given by [9]

$$Z_{Ylj} = \left(1 - \frac{\partial \langle Y|\Delta\Sigma_{lj}(E)|Y\rangle}{\partial E}\bigg|_{\epsilon_{Ylj}^{qh}}\right)^{-1}. \qquad (19)$$

Finally, the continuum contribution of Eq. (16) and the quasihole parts of Eq. (18), which are obtained in the basis of box states, can be added and renormalized to obtain the spectral function in the continuum representation at the momenta defined by Eq. (11):

$$S_{lj}(p_m, p_n; E) = \frac{2}{\pi} \frac{1}{N_{il}^2} \left(\widetilde{S}_{lj}^c(p_m, p_n; E)\right.$$
$$\left. + \sum_Y \widetilde{S}_{Ylj}^{qh}(p_m, p_n; E)\right). \qquad (20)$$

It is useful to have a separable representation of the spectral function in momentum space. For a given energy, the spectral function in the box is represented by a matrix in momentum space; after diagonalizing this matrix, one obtains

$$S_{lj}(p_m, p_n; E) = \sum_i^{N_{max}} S_{lj}(i)\phi_i(p_m)\phi_i(p_n), \qquad (21)$$

where $S_{lj}(i)$ are the eigenvalues and ϕ_i are the corresponding eigenfunctions. In all cases considered here, it is enough to consider the first five or six largest eigenvalues in Eq. (21) for an accurate representation of the spectral function. These eigenfunctions are in principle sp overlap functions [see discussion after Eq. (29) below]. They can be thought of as the natural orbits at a given energy. In fact, if the diagonalization is performed after integrating over the energy E, one would precisely obtain the natural orbits associated with the one-body density matrix and the eigenvalues $S_{lj}(i)$ would be the natural occupation numbers [10].

III. GENERAL FORMALISM OF THE DWIA

For the scattering of an ultrarelativistic electron with initial (final) momentum $\mathbf{p}_e(\mathbf{p}'_e)$, while a nucleon is ejected with final momentum $\mathbf{p}'_N$, the differential cross section in the one-photon-exchange approximation reads [19,21]

$$\frac{d\sigma}{d\mathbf{p}'_e d\mathbf{p}'_N} = \frac{e^4}{16\pi^2} \frac{1}{Q^4 p_e p'_e} \sum_{\lambda,\lambda'=0,\pm 1} L_{\lambda,\lambda'} W_{\lambda,\lambda'}, \quad (22)$$

where $Q^2 = \mathbf{q}^2 - \omega^2$ and $\mathbf{q} = \mathbf{p}_e - \mathbf{p}'_e$, $\omega = p_e - p'_e$ are the momentum and energy transferred to the target nucleus, respectively. The quantities $L_{\lambda,\lambda'}$, $W_{\lambda,\lambda'}$ (usually referred to as the lepton and hadron tensors, respectively) are expressed in the basis of unit vectors

$$e_0 = (1,0,0,0),$$
$$e_{\pm 1} = \left(0, \mp\sqrt{\frac{1}{2}}, -\sqrt{\frac{1}{2}}i, 0\right), \qquad (23)$$

which define the longitudinal (0) and transverse (± 1) components of the nuclear response with respect to the polarization of the exchanged virtual photon. The components of the lepton tensor depend only on the electron kinematics, while

$W_{\lambda,\lambda'}$ depend on q, ω, p'_N, $\cos\gamma = \mathbf{p}'_N \cdot \mathbf{q}/p'_N q$, and the angle α between the $(\mathbf{p}'_N, \mathbf{q})$ plane and the electron scattering plane.

The hadron tensor is defined as [19,21,33]

$$W_{\lambda,\lambda'} = \overline{\sum_i} \sum_f J_\lambda(\mathbf{q})J_{\lambda'}^*(\mathbf{q})\delta(E_i - E_f); \qquad (24)$$

i.e., it involves the average over initial states and the sum over the final undetected states (compatible with energy-momentum conservation) of bilinear products of the scattering amplitude $J_\lambda(\mathbf{q})$.

This basic ingredient of the calculation is defined as

$$J_\lambda(\mathbf{q}) = \int d\mathbf{r}\, e^{i\mathbf{q}\cdot\mathbf{r}} \langle\Psi_f^A|\hat{J}_\mu \cdot e_\lambda^\mu|\Psi_0^A\rangle, \qquad (25)$$

where the matrix element of the nuclear charge-current density operator $\hat{J}_\mu$ is taken between the initial, $|\Psi_0^A\rangle$, and the final, $|\Psi_f^A\rangle$, nuclear states. A natural choice for $|\Psi_f^A\rangle$ is suggested by the experimental conditions of the reaction selecting a final state, which behaves asymptotically as a knocked-out nucleon with momentum p'_N and a residual nucleus in a well-defined state $|\Psi_n^{A-1}(E)\rangle$ with energy E and quantum numbers n. By projecting this specific channel out of the entire Hilbert space, it is possible to rewrite Eq. (25) in a one-body representation (in momentum space and omitting spin degrees of freedom for simplicity) as [18]

$$J_\lambda(\mathbf{q}) = \int d\mathbf{p}\, \chi_{p'_N En}^{(-)*}(\mathbf{p}+\mathbf{q})\hat{J}_\mu^{eff}(\mathbf{p},\mathbf{q}) \cdot e_\lambda^\mu \phi_{En}(\mathbf{p})[S_n(E)]^{1/2}, \qquad (26)$$

provided that $\hat{J}_\mu$ is substituted by an appropriate effective one-body charge-current density operator $\hat{J}_\mu^{eff}$, which guarantees the orthogonality between $|\Psi_0^A\rangle$ and $|\Psi_f^A\rangle$ besides taking into account effects due to truncation of the Hilbert space. Actually, the orthogonality defect is negligible in the standard kinematics for $(e,e'p)$ reactions and in the DWIA $\hat{J}_\mu^{eff}$ is usually replaced by a simple one-body current operator [18,20,21].

The functions

$$[S_n(E)]^{1/2}\phi_{En}(\mathbf{p}) = \langle\Psi_n^{A-1}(E)|a(\mathbf{p})|\Psi_0^A\rangle,$$
$$\chi_{p'_N En}^{(-)}(\mathbf{p}) = \langle\Psi_n^{A-1}(E)|a(\mathbf{p})|\Psi_f^A\rangle \qquad (27)$$

describe the overlap between the residual state $|\Psi_n^{A-1}(E)\rangle$ and the hole produced in $|\Psi_0^A\rangle$ and $|\Psi_f^A\rangle$, respectively, by removing a particle with momentum $\mathbf{p}$. Both $\phi_{En}, \chi_{p'_N En}^{(-)}$ are eigenfunctions of a Feshbach-like nonlocal energy-dependent Hamiltonian referred to the residual nucleus, belonging to the eigenvalues E and $E+\omega$, respectively [17]. The norm of ϕ_{En} is 1 and $S_n(E)$ is the spectroscopic factor associated with the removal process; i.e., it is the probability that the residual nucleus can indeed be conceived as a hole produced in the target nucleus. The dependence of $\chi_{p'_N En}^{(-)}$ on

p'_N is hidden in the asymptotic state $|\Psi^A_f\rangle$ and the boundary conditions are those of an incoming wave.

Because of the complexity of the eigenvalue problem in the continuum, the Feshbach Hamiltonian is usually replaced by a phenomenological local optical potential $V(\mathbf{r})$ of the Woods-Saxon form with complex central and spin-orbit components. It simulates the mean-field interaction between the residual nucleus and the emitted nucleon with energy-dependent parameters determined through a best fit of elastic nucleon-nucleus scattering data including cross section and polarizations. Then, $\chi^{(-)}_{p'_N En} \sim \chi^{(-)}_{p'_N}$ is expanded in partial waves and a Schrödinger equation including $V(\mathbf{r})$ is solved for each component up to a maximum angular momentum satisfying a p'_N-dependent convergency criterion [21]. The nonlocality of the original Feshbach Hamiltonian is taken into account by multiplying the optical-model solution by the appropriate Perey factor [34].

After summing over the undetected final states with quantum numbers n of the residual nucleus, the hadron tensor $W_{\lambda,\lambda'}$ in momentum space becomes

$$W_{\lambda,\lambda'} \sim \sum_n \int d\mathbf{p} d\mathbf{p}' \chi^{(-)*}_{p'_N}(\mathbf{p}+\mathbf{q}) \hat{J}_\mu(\mathbf{p},\mathbf{q}) \cdot e^\mu_\lambda \phi_{En}(\mathbf{p})$$

$$\times \phi^*_{En}(\mathbf{p}') S_n(E) \hat{J}^\dagger_\nu(\mathbf{p}',\mathbf{q}) \cdot e^{\nu\dagger}_{\lambda'} \chi^{(-)}_{p'_N}(\mathbf{p}'+\mathbf{q})$$

$$\equiv \int d\mathbf{p} d\mathbf{p}' \chi^{(-)*}_{p'_N}(\mathbf{p}+\mathbf{q}) \hat{J}_\mu(\mathbf{p},\mathbf{q}) \cdot e^\mu_\lambda S(\mathbf{p},\mathbf{p}';E)$$

$$\times \hat{J}^\dagger_\nu(\mathbf{p}',\mathbf{q}) \cdot e^{\nu\dagger}_{\lambda'} \chi^{(-)}_{p'_N}(\mathbf{p}'+\mathbf{q}), \qquad (28)$$

where

$$S(\mathbf{p},\mathbf{p}';E) = \sum_n S_n(E) \phi^*_{En}(\mathbf{p}') \phi_{En}(\mathbf{p}) \qquad (29)$$

is the hole spectral function defined in Eq. (1). Notice that the spin and isospin indices have been omitted for simplicity and the summation over n is over the different partial wave contributions which are present at a given energy E. This sum should not be confused with the separable representation [Eq. (21)] of the partial wave contributions to the spectral function $S_{lj}(p,p',E)$ defined in Eq. (2). Each lj contribution, coming from either quasihole states (if E is the correct excitation energy) or from states which are usually unoccupied in the standard shell model, can be separately computed, so that the total hadron tensor will look like

$$W_{\lambda,\lambda'} \equiv \sum_{lj} W^{lj}_{\lambda,\lambda'}. \qquad (30)$$

Experimental data for the $(e,e'p)$ reaction are usually collected as ratios between the measured cross section and $K\sigma_{eN}$, where K is a suitable kinematical factor and σ_{eN} is the elementary (half off-shell) electron-nucleon cross section. In this way the information contained in the fivefold differential cross section is reduced to a twofold function of the missing energy $E_m = \omega - T_{p'_N} - E_x$ ($T_{p'_N}$ is the kinetic energy of the emitted nucleon and E_x is the excitation energy of the residual nucleus) and of the missing momentum
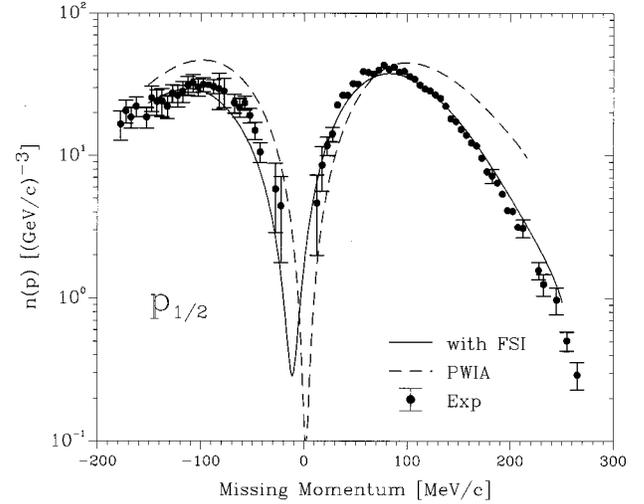

FIG. 2. Reduced cross section for the ^{16}O$(e,e'p)^{15}$N$_{\text{g.s.}}$ reaction in parallel kinematics. Results with (solid line) and without (dashed line) inclusion of the FSI's are compared to the experimental data [5]. A spectroscopic factor of 0.644 has been employed in displaying the results for the calculations involving the spectral function.

$\mathbf{p}_m = \mathbf{p}'_N - \mathbf{q}$ [1]. Therefore, in the following section results will be presented under the form of the so-called reduced cross section [21]

$$n(\mathbf{p}_m) \equiv \frac{d\sigma}{d\mathbf{p}'_e d\mathbf{p}'_N} \frac{1}{K\sigma_{eN}}. \qquad (31)$$

IV. RESULTS

In this section we will discuss results for the reduced cross section defined in Eq. (31) for $(e,e'p)$ reactions on ^{16}O leading both to discrete bound states of the residual nucleus ^{15}N and to states in the continuum at higher missing energy. Distortion of electron and proton waves has been taken into account through the effective momentum approximation [35] and through the optical potential derived from the Schwandt parametrization [36] (see Table III in Ref. [5]), respectively. All results presented here have been obtained using the CC1 prescription [37] for the half off-shell elementary electron-proton scattering amplitude in analogy with what has been commonly done in the analysis of the experimental data. We also employed the nonrelativistic description for this amplitude [38] to be consistent with the nonrelativistic calculation of the fivefold differential cross section. In parallel kinematics, where most of the experimental data are available, this choice does not produce very different results with respect to the former and, therefore, will not be considered in the following.

A. Quasihole states

In Fig. 2 the experimental results for the transition to the ground state of ^{15}N are displayed as a function of the missing momentum $\mathbf{p}_m$. These data points have been collected at NIKHEF choosing the so-called parallel kinematics [5], where the direction of the momentum of the outgoing proton, $\mathbf{p}'_N$, has been fixed to be parallel to the momentum transfer

q. In order to minimize the effects of the energy dependence of the optical potential describing FSI's, the data points have been collected at a constant kinetic energy of 90 MeV in the center-of-mass system of the emitted proton and the residual nucleus. Consequently, since the momentum of the ejected particle is also fixed and

$$p_m = |p'_N| - |q|, \qquad (32)$$

the missing momentum can be modified by collecting data at various momenta q transferred from the scattered electron.

The experimental data points for this reduced cross section are compared to the predictions of the calculations discussed above. The quasihole part of the spectral function for the $p\frac{1}{2}$ partial wave represents the relevant piece of the nuclear structure calculation for the proton knockout reaction leading to the ground state of ^{15}N. Using the quasihole part of the spectral function as discussed above [see Eq. (18)] but adjusting the spectroscopic factor for the quasihole state contribution $Z_{0p1/2}$ to fit the experimental data, we obtain the solid line of Fig. 2. Comparing this result with the experimental data one one finds that the calculated spectral function reproduces the shape of the reduced cross section as a function of the missing momentum very well. The absolute value for the reduced cross section can only be reproduced by assuming a spectroscopic factor $Z_{0p1/2} = 0.644$, a value considerably below the one of 0.89 calculated from Eq. (19) [9]. The phenomenological Woods-Saxon wave functions adjusted to fit the shape of the reduced cross section require spectroscopic factors ranging from 0.61 to 0.64 for the lowest $0p\frac{1}{2}$ state and from 0.50 to 0.59 for the $0p\frac{3}{2}$ state, respectively, depending upon the choice of the optical potential for the outgoing proton [5]. The fact that the calculated spectroscopic factor is larger than the one adjusted to the experimental data may be explained by the observation that the calculations only reflect the depletion of the quasihole occupation due to short-range correlations. Further depletion and fragmentation should arise from long-range correlations due to collective excitations at low energies [6,31]. Other explanations for this discrepancy could be the need for improving the description of spurious center-of-mass motion [39,7] or a different treatment of FSI's in terms of a relativistic model for the optical potential [40].

In order to visualize the effects of FSI's, Fig. 2 also displays the results obtained for the quasihole contribution to the spectral function (with the same spectroscopic factor $Z_{0p1/2} = 0.644$ as before, for the sake of consistency) but ignoring the effects of the optical potential. In this so-called plane-wave impulse approximation (PWIA) the reduced cross section as a function of the missing momentum is identical to the spectral function at the missing energy of the considered $0p\frac{1}{2}$ state or, better, to the momentum distribution of the peak observed at this missing energy with the quantum numbers of the ground state of ^{15}N. Therefore, the difference between the solid and dashed lines in Fig. 2 corresponds to the difference between the reduced cross section defined in Eq. (31) and the momentum distribution for the ground state of ^{15}N. In other words, it illustrates the effect of all the ingredients entering the present theoretical description of the $(e,e'p)$ reaction, which are not contained in the calculation of the spectral function. In particular, the real part of the
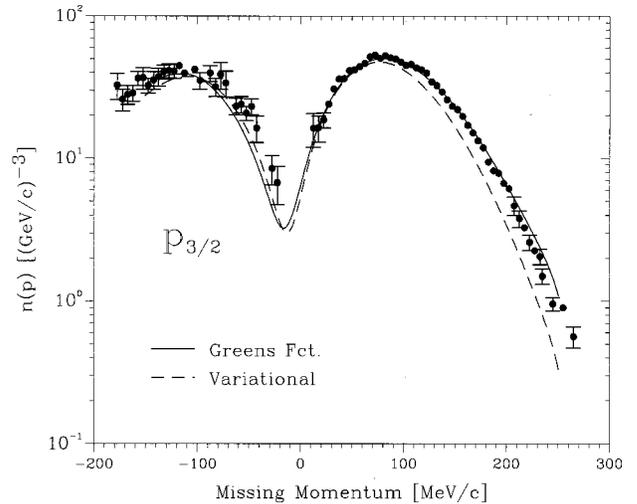

FIG. 3. Reduced cross section for the ^{16}O$(e,e'p)$ reaction in parallel kinematics leading to the $\frac{3}{2}^-$ state at -6.32 MeV of the residual nucleus ^{15}N. Results of the present Green's function approach (solid line) are compared to those obtained in the variational calculation of [7] (dashed line) and the experimental data [5]. A spectroscopic factor of 0.537 was required for the Green's function approach, while $Z_{p3/2} = 0.459$ has been used to adjust the results of the variational calculation.

optical potential yields a reduction of the momentum of the outgoing proton p'_N. According to Eq. (32), this implies in parallel kinematics a redistribution of the strength towards smaller values of the missing momentum and makes it possible to reproduce the observed asymmetry of the data around $p_m = 0$. This feature cannot be obtained in the PWIA (dashed line), where the results are symmetric around $p_m = 0$ due to the cylindrical symmetry of the hadron tensor $W_{\lambda,\lambda'}$ around the direction of **q** when FSI's are switched off (for a general review see Ref. [21] and references therein). The imaginary part of the optical potential describes the absorption of the proton flux due to coherent inelastic rescatterings, which produces the well known quenching with respect to the PWIA result.

As a second example for the reduced cross section in $(e,e'p)$ reactions on ^{16}O leading to bound states of the residual nucleus, we present in Fig. 3 the data for the $\frac{3}{2}^-$ state of ^{15}N at an excitation energy of -6.32 MeV. Also in this case the experimental data are reproduced very well if we adjust the spectroscopic factor for the corresponding quasihole part in the spectral function to $Z_{0p3/2} = 0.537$. The discrepancy with the calculated spectroscopic factor (0.914) is even larger for this partial wave than it is for the $p\frac{1}{2}$ state. A large part of this discrepancy can be attributed to long-range correlations, which are not accounted for in the present study. Note that in the experimental data three $\frac{3}{2}^-$ states are observed in ^{15}N at low excitation energies. Long-range correlations yield a splitting such that 86% of the total strength going to these three states is contained in the experimental data displayed in Fig. 3. This splitting is not observed in the theoretical calculations. If one divides the adjusted spectroscopic factor $Z_{0p3/2}$ by 0.86 to account for the splitting of the experimental strength, one obtains a value of 0.624 which is
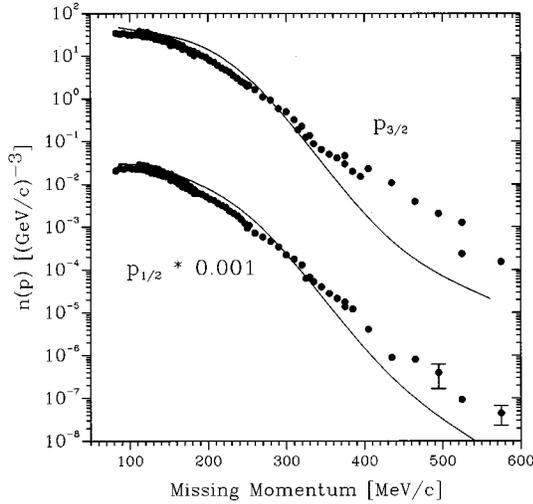
FIG. 4. Reduced cross section for the ^{16}O$(e,e'p)$ reaction leading to the ground and the $\frac{3}{2}^-$ states of ^{15}N in the kinematical conditions considered in the experiment of [15]. The calculations were performed using the same spectral functions as discussed for Figs. 2 and 3.

close to the total spectroscopic factor adjusted to describe the knockout of a proton from a $p\frac{1}{2}$ state.

Figure 3 also contains the results for the reduced cross section derived by substituting the overlap $[S_n(E)]^{1/2}\phi_{En}$ in Eq. (26) with the variational wave function of Radici *et al.* [7], who employed the Argonne potential for the NN interaction [41]. Also in this case the shape of the experimental data is globally reproduced with a slightly better agreement for small negative values of p_m but with a clear underestimation at larger p_m. The overall quality of the fit is somewhat worse than for the Green's function approach and the required adjusted spectroscopic factor is $Z_{0p3/2}=0.459$, even below the value of 0.537 needed in the present calculation. It is not clear, however, whether the differences in the calculated reduced cross section are more due to the use of different interactions or more to the various methods employed in calculating the spectral function.

The analysis of the reduced cross section has been extended to higher missing momenta by experiments performed at the MAMI accelerator in Mainz [15], adopting different kinematical conditions than the parallel kinematics. Using the same spectroscopic factors for the $p\frac{3}{2}$ and the $p\frac{1}{2}$ partial waves, which were adjusted to the NIKHEF data above, the results of our calculations agree quite well also with these MAMI data, as displayed in Fig. 4. Although the calculation is somewhat below the data at high missing momentum, one should keep in mind that the corresponding difference in sp strength is only an extremely tiny fraction of the 10% of the protons which are expected to be associated with high momenta due to short-range correlations [8–10].

B. Contribution of the continuum

From theoretical studies it is known that an enhancement of the high-momentum components due to short-range NN correlations does not show up in knockout experiments leading to states of low excitation energy in the $(A-1)$ nucleus, but should be seen at higher missing energies, which corre-

spond to large excitation energies in the residual nucleus. A careful analysis of such reactions leading to final states above the threshold for two-nucleon emission, however, is much more involved. For example, a description of the electromagnetic vertex beyond the impulse approximation is needed and two-body current operators must be adopted which are consistent with the contributions included in the spectral function. Moreover, the possible further fragmentation of the $(A-1)$ residual system requires, for a realistic description of FSI's, a coupled-channel formalism with many open channels. Calculations based on the optical potential are not satisfactory at such missing energies, because inelastic rescatterings and multistep processes will add and remove strength from this particular channel.

Nevertheless, it should be of interest to analyze the predictions of the present approach at such missing energies, first of all, because it represents the first realistic attempt of a complete calculation of the single-particle channel leading to the final proton emission, including intermediate states above the Fermi level up to $l=4$, and therefore, it represents a realistic estimate of the relative size of this specific channel; second, because information on the shape of the reduced cross section as a function of the missing momentum or on the relative contribution of various partial waves could yield reliable results even at these missing energies. Because of the problems mentioned above, no reliable description of the absolute value of the reduced cross section can be reached in this framework.

In order to demonstrate the energy dependence of the spectral function and its effect on the cross section, we have calculated the reduced cross section for the excitation of $\frac{3}{2}^-$ states at $E_m=-63$ MeV. For these studies we considered the so-called perpendicular kinematics, where the energy of the emitted proton is kept fixed at 90 MeV as well as the momentum transfer at $q\sim420$ MeV/c (equal to the outgoing proton momentum). The same optical potential as in Figs. 2 and 3 can be adopted to describe FSI's and the missing momentum distribution is obtained by varying the angle between $\mathbf{p}'_N$ and $\mathbf{q}$. For a spectral function normalized to unity (as the absolute result for the cross section is not reliable), the reduced cross section is represented by the solid line in Fig. 5. If, however, we replace the spectral function derived from the continuum contribution in Eq. (20) by the one derived for the $\frac{3}{2}^-$ quasihole state at its proper missing energy (but now in the same kind of perpendicular kinematics and normalized to 1), we obtain the dashed line. A comparison of these two calculations demonstrates the enhancement of the high-momentum components in the spectral function leading to final states at large excitation energies. Note that the cross section derived from the appropriate spectral function is about two orders of magnitude larger at $p_m\sim500$ MeV/c than the one derived from the spectral function at the quasihole energy.

The discussion so far is of course somewhat academic since it will be difficult to perform a decomposition of the continuum contribution to the reduced cross section in terms of the quantum numbers for angular momentum and parity of the state for the residual system. Therefore we display in Figs. 6 and 7 the contributions to the total reduced cross section of the various partial waves associated with states above the Fermi level and usually unoccupied in the standard
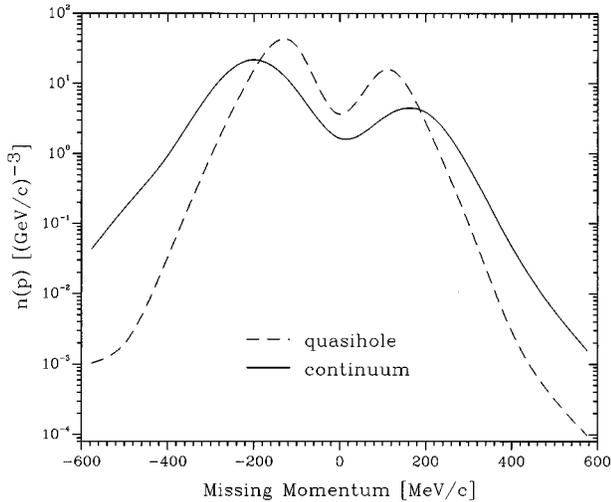
FIG. 5. Reduced cross section for the $^{16}O(e,e'p)$ reaction in perpendicular kinematics for the excitation of $\frac{3}{2}^-$ states at $E_m = -63$ MeV (solid line) and -6.32 MeV (dashed line).

shell model. From Fig. 6 we can furthermore see that the relative importance of the various partial waves changes with the missing momentum, emphasizing the contribution of higher angular momenta at increasing p_m. This feature can be observed even better in Fig. 7, where the percentage of each relative contribution to the total reduced cross section is displayed as a function of the missing momentum. For each orbital angular momentum we obtain a "window" in p_m where its contribution shows a maximum as compared to other partial waves.

V. CONCLUSIONS

In the present paper the consequences of the presence of high-momentum components in the ^{16}O ground state have been explored in the calculation of the $(e,e'p)$ cross section within the formalism for the DWIA developed in Refs. [17–22]. The spectral functions have been calculated for the
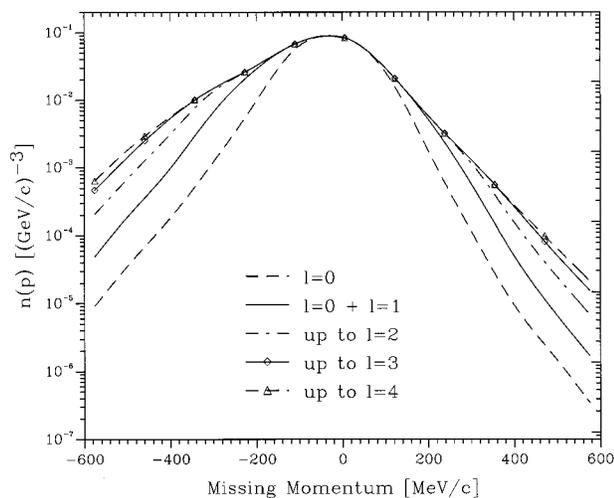

FIG. 6. Contributions of various partial waves to the reduced cross section for the $^{16}O(e,e'p)$ reaction in the same conditions as for the solid line in Fig. 5.
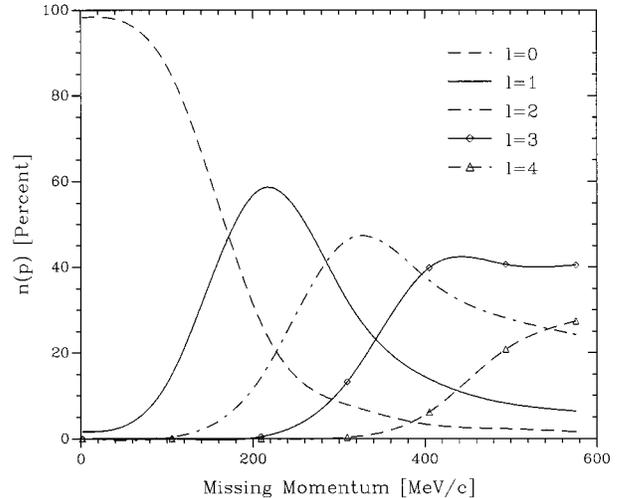

FIG. 7. Relative importance of various partial waves to the reduced cross section for the $^{16}O(e,e'p)$ reaction in the same conditions as in Fig. 6.

^{16}O system itself, by employing the techniques developed and discussed in [26,8–10]. At low missing energies, the description of the missing momentum dependence of the $p\frac{1}{2}$ and $p\frac{3}{2}$ quasihole states compares favorably with the experimental data obtained at NIKHEF [5] and at the MAMI facility in Mainz [15]. The difference between theory and experiment at high missing momenta can at most account for a very tiny fraction of the sp strength which is predicted to be present at these momenta [8–10]. A comparison with the PWIA result clarifies the influence of FSI's in parallel kinematics. We also compare our results for the $p\frac{3}{2}$ quasihole state with the results obtained in Ref. [7] for the Argonne NN interaction. While the shape of the cross sections is nicely described by our results, the associated spectroscopic factors are overestimated substantially. Although a large fraction of this discrepancy can be ascribed to the influence of long-range correlations [6,31], which are outside the scope of the present work, a discrepancy may still remain, although it has been suggested that a correct treatment of the center-of-mass motion [7] may fill this gap.

As discussed previously for nuclear matter (see, e.g., [13]) and emphasized in [8–10] for finite nuclei, the admixture of high-momentum components in the nuclear ground state can only be explored by considering high missing energies in the $(e,e'p)$ reaction. Although other processes may contribute to the cross section at these energies, we have demonstrated in this paper that the expected emergence of high-missing-momentum components in the cross section is indeed obtained and yields substantially larger cross sections than the corresponding outcome for the quasihole states. As a result, we conclude that the presence of high-momentum components leads to a detectable cross section at high missing energy. In addition, we observe that it is important to include orbital angular momenta at least up to $l=4$ in the spectral function in order to account for all the high-missing-momentum components up to about 600 MeV/c. A clear window for the dominant contribution of each l value as a function of missing momentum is also established. This feature may help to analyze experimental data at these high missing energies.

[1] P. K. A. de Witt Huberts, J. Phys. G **16**, 507 (1990); G. van der Steenhoven, Nucl. Phys. **A527**, 17c (1991); L. Lapikás, *ibid.* **A553**, 297c (1993).

[2] G. J. Wagner, in *Nuclear Structure at High Spin, Excitation, and Momentum Transfer*, edited by Hermann Mann, AIP Conf. Proc. No. 142 (AIP, New York, 1982), p. 220; P. Grabmayr *et al.*, Phys. Lett. **164B**, 15 (1985).

[3] W. H. Dickhoff and H. Müther, Rep. Prog. Phys. **55**, 1947 (1992).

[4] C. Mahaux and R. Sartor, Adv. Nucl. Phys. **20**, 1 (1991).

[5] M. Leuschner *et al.*, Phys. Rev. C **49**, 955 (1994).

[6] W. J. W. Geurts, K. Allaart, W. H. Dickhoff, and H. Müther, Phys. Rev. C **53**, 2207 (1996).

[7] M. Radici, S. Boffi, S. C. Pieper, and V. R. Pandharipande, Phys. Rev. C **50**, 3010 (1994).

[8] H. Müther and W. H. Dickhoff, Phys. Rev. C **49**, R17 (1994).

[9] H. Müther, A. Polls, and W. H. Dickhoff, Phys. Rev. C **51**, 3040 (1995).

[10] A. Polls, H. Müther, and W. H. Dickhoff, Nucl. Phys. **A594**, 117 (1995).

[11] I. Sick, S. Fantoni, A. Fabrocini, and O. Benhar, Phys. Lett. B **323**, 267 (1994).

[12] D. Van Neck, A. E. L. Dieperink, and E. Moya de Guerra, Phys. Rev. C **51**, 1800 (1995).

[13] C. Ciofi degli Atti, S. Simula, L. L. Frankfurt, and M. I. Strikman Phys. Rev. C **44**, R7 (1991).

[14] I. Bobeldijk *et al.*, Phys. Rev. Lett. **73**, 2684 (1994).

[15] K. I. Blomqvist *et al.*, Phys. Lett. B **344**, 85 (1995).

[16] C. Giusti and F. D. Pacati, Nucl. Phys. **A336**, 427 (1980).

[17] S. Boffi and F. Cappuzzi, Nucl. Phys. **A351**, 219 (1981).

[18] S. Boffi, F. Cannata, F. Capuzzi, C. Giusti, and F. D. Pacati, Nucl. Phys. **A379**, 509 (1982).

[19] S. Boffi, C. Giusti, and F. D. Pacati, Nucl. Phys. **A386**, 599 (1982).

[20] S. Boffi and M. Radici, Nucl. Phys. **A526**, 602 (1991).

[21] S. Boffi, C. Giusti, and F. D. Pacati, Phys. Rep. **226**, 1 (1993).

[22] S. Boffi, C. Giusti, F. D. Pacati, and M. Radici, *Electromagnetic Response of Atomic Nuclei* (Oxford University Press, Oxford, 1996).

[23] R. Machleidt, Adv. Nucl. Phys. **19**, 1 (1989).

[24] D. Bonatsos and H. Müther, Nucl. Phys. **A496**, 23 (1989).

[25] C. W. Wong and D. M. Clement, Nucl. Phys. **A183**, 210 (1972).

[26] M. Borromeo, D. Bonatsos, H. Müther, and A. Polls, Nucl. Phys. **A539**, 189 (1992).

[27] M. G. E. Brand, G. A. Rijsdijk, F. A. Muller, K. Allaart, and W. H. Dickhoff, Nucl. Phys. **A531**, 253 (1991).

[28] G. A. Rijsdijk, K. Allaart, and W. H. Dickhoff, Nucl. Phys. **A550**, 159 (1992).

[29] H. Müther and L. D. Skouras, Phys. Lett. B **306**, 306 (1993).

[30] H. Müther and L. D. Skouras, Nucl. Phys. **A581**, 247 (1995).

[31] K. Amir-Azimi-Nili, H. Müther, L. D. Skouras, and A. Polls, Nucl. Phys. **A604**, 245 (1996).

[32] C. Mahaux, P. F. Bortignon, R. A. Broglia, and C. H. Dasso, Phys. Rep. **120**, 1 (1985).

[33] S. Frullani and J. Mougey Adv. Nucl. Phys. **13**, 1 (1984).

[34] F. G. Perey, in *Direct Interactions and Nuclear Reaction Mechanism,* edited by E. Clementel and C. Villi (Gordon and Breach, New York, 1963), p. 125; F. Capuzzi, Lecture Notes in Physics Vol. 55 (Springer-Verlag, Berlin, 1976), p. 20.

[35] C. Giusti and F. D. Pacati, Nucl. Phys. **A473**, 717 (1987); A485, 461 (1988).

[36] P. Schwandt *et al.*, Phys. Rev. C **26**, 55 (1982).

[37] T. de Forest, Jr., Nucl. Phys. **A392**, 232 (1983).

[38] V. Devanathan, Ann. Phys. (N.Y.) **43**, 74 (1967).

[39] S. C. Pieper, R. B. Wiringa, and V. R. Pandharipande, Phys. Rev. C **46**, 1741 (1992).

[40] J. M. Udias, P. Sarriguren, E. Moya de Guerra, E. Garrido, and J. A. Caballero, Phys. Rev. C **51**, 3246 (1995).

[41] R. B. Wiringa, R. A. Smith, and T. L. Ainsworth, Phys. Rev. C **29**, 1207 (1984).